A modeling framework to assess the crop production potential of green roofs

Xie, P.; Barbarossa, V.; Erisman, J.W.; Mogollón, J.M.

Science of the Total Environment 907 (2024) 168051

Contents lists available at ScienceDirect

Science of the Total Environment

journal homepage: www.elsevier.com/locate/scitotenv

A modeling framework to assess the crop production potential of green roofs

Pengxuan Xie [a,*], Valerio Barbarossa [a,b], Jan Willem Erisman [a], José M. Mogollón [a]

[a] Institute of Environmental Sciences (CML), Leiden University, P.O. Box 9518, 2300 RA Leiden, the Netherlands
[b] PBL Netherlands Environmental Assessment Agency, Department of Nature and Rural Areas, The Hague, the Netherlands

HIGHLIGHTS

- A new spatially-explicit modeling framework to explore food production potential on green roofs using a crop model.
- Implementing an optimized irrigation strategy for crop growth is important for green roof food production estimates.
- The Aquacrop model works well to simulate different shallow-rooted types of crops on green roofs.
- Amsterdam has a potential green roof area of ~400 ha that can produce up to nearly 28 thousand tons of food.

GRAPHICAL ABSTRACT

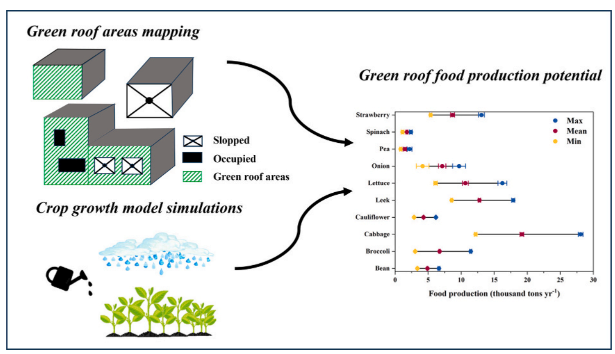

ARTICLE INFO

Editor: Charlotte Poschenrieder

Keywords:
Potential green roof areas
Spatial analysis
Crop model
Water use efficiency
Optimized irrigation strategy

ABSTRACT

The increase in food demand and limited opportunities to expand agricultural land pose a threat to local and global food security. Producing food in urban areas such as green roofs can help satisfy urban food demand and thus alleviate pressure on agricultural land. However, a modeling framework that simulates crop growth and production potential on green roofs at a city scale is missing. Here, we adapt the Aquacrop model to explore the growth potential of various types of crops on green roofs and apply it to suitable roof areas in the city of Amsterdam. Our modeling framework includes irrigation methods for water use on green roofs that are optimized according to various climate-driven scenarios of water availability. We find that cabbage has the maximum achievable crop yields ranging from 30.8 to 75.9 t ha^{-1} yr^{-1}, while pea has the minimum achievable crop yields ranging from 1.7 to 6.4 t ha^{-1} yr^{-1}. The potential suitable green roof area (i.e., roofs with a certain slope and bearing capacity) for Amsterdam is roughly 400 ha for crop production. This represents 16 % of the total rooftop areas of Amsterdam and can produce up to a total of 28 kt of crops on an annual basis. Our modeling framework can be easily applied to other cities to identify the crop growth potential of green roofs. Our results can help policymakers and urban planners find optimal planting strategies and contribute to shorter food supply chains.

* Corresponding author.
E-mail address: p.xie@cml.leidenuniv.nl (P. Xie).

https://doi.org/10.1016/j.scitotenv.2023.168051
Received 18 July 2023; Received in revised form 27 September 2023; Accepted 21 October 2023
Available online 28 October 2023

1. Introduction

With an expected continued population growth, food demand will keep increasing in the coming decades (Godfray et al., 2010; Foley et al., 2011; FAO, 2018). Meanwhile, urban areas will likely expand into peri-urban farmland, affecting up to 4 % of annual food production by 2030 (Bren d'Amour et al., 2017). More broadly, changes in diets, the reduction in the quality of agricultural land, and increasing food waste can also put additional pressure on food production (Tian et al., 2021). Urban food production may contribute to solving these problems by integrating food production systems into urban spaces while profiting from the nutrients found in urban waste to produce a variety of crops (Smit et al., 1996). Roofs suitable for agricultural production represent 21 %–26 % of urban areas (Getter and Rowe, 2006), and thus hold great potential for urban food production.

Many studies have explored the crop production potential on green roofs, including at the building, urban, and global scales. At the building scale, crop yields are usually assessed using biogeochemical models, statistical data, and/or experimental data. For instance, Jing et al. (2021) simulated annual yields for seven crops (lettuce, broccoli, tomato, cabbage, potato, radish, and celery) on green roofs under various growing conditions using a Denitrification-Decomposition (DNDC), and found that lettuce had the maximum crop yields ranging from 117 to 255 t ha^{-1} while potato had the minimum crop yields ranging from 6 to 12 t ha^{-1}. Models that combine irrigation with crop yields spatially, such as the distributed Aquacrop model, are being increasingly used in agricultural studies to explore the food production potential and water use requirements (Han et al., 2020; Manivasagam and Rozenstein, 2020; Liu and Yang, 2021). The feasibility of the Aquacrop model has been shown for different vegetable types (e.g., lettuce, cabbage, pea, and onion) (Wellens et al., 2013; Pérez-Ortolá et al., 2014; Paredes and Torres, 2016; Ćosić et al., 2017; Ket et al., 2018). Yet, combining Aquacrop model simulations with spatial information to explore the food production potential on green roofs has not yet been tested.

To explore their food production potential, green roof areas suitable for crop planting need to be determined, which may depend on various green roof criteria (Nadal et al., 2017; Zambrano-Prado et al., 2021; Montealegre et al., 2022). For instance, Saha and Eckelman (2017) estimated that a potential green roof area of 922 ha (corresponding to 42 % of the entire rooftop space of Boston) is available for food production by identifying suitable roof areas through a Digital Surface Model (DSM). These potential green roof area estimates are then coupled to statistical and/or experimental data to evaluate regional food production potential on green roofs (e.g. Meng et al., 2022; Meng et al., 2023). Following such an approach, Zambrano-Prado et al. (2021) identified 8 % (0.2 km^2) of total roofs as potential green roof areas in a region north of Barcelona, which could provide food for over 140,000 people on average, or 210 % of the population in the study region. Furthermore, Orsini et al. (2014) estimated 3500 flat rooftops in Bologna, with a flat area of around 82 ha, and via experiments estimated that Bologna's green roofs could produce about 13 kt y^{-1} of vegetables. With world urban green areas totaling 7.1–11.3 million hectares, Clinton et al. (2018) anticipated a possible annual global food production of 100–180 million t from statistical data, with green roofs accounting for 11.0 %–19.4 % of those urban green areas.

Here, we develop a framework to assess the crop production potential of green roofs using the Aquacrop model. We use this framework to simulate crop yields on green roofs and apply the model at a city scale (i.e., the urban area of Amsterdam). We selected 10 crops for our study, including lettuce, cabbage, onion, pea, leek, strawberry, spinach, cauliflower, bean, and broccoli, based on their shallow-rooted systems, making them suitable for cultivation within a 20 cm deep lightweight soil, such as the one used on green roofs. These crops not only play a significant role in Amsterdam's vegetable production (strawberries are also classified as vegetable by Statistics Netherlands (CBS)) but also contribute to 82.5 % of the Netherlands' total vegetable output, amounting to 2.7 Mt of open-air production in 2020 (CBS, 2022). In our modeling framework, we (i) identify potential green roof areas suitable for crop planting using Geographic Information Systems (GIS), (ii) estimate distributed crop yields on green roofs using the Aquacrop model in combination with gridded climate information and variable management practices, and (iii) quantify the green roof production potential by combining Aquacrop simulations with green roof potential suitable areas estimates.

2. Methods

2.1. Study area

Amsterdam, the Netherlands, is an ideal location to examine the crop production potential for green roofs as (i) a high-resolution Digital Surface Model (DSM), essential for estimating the potential green roof

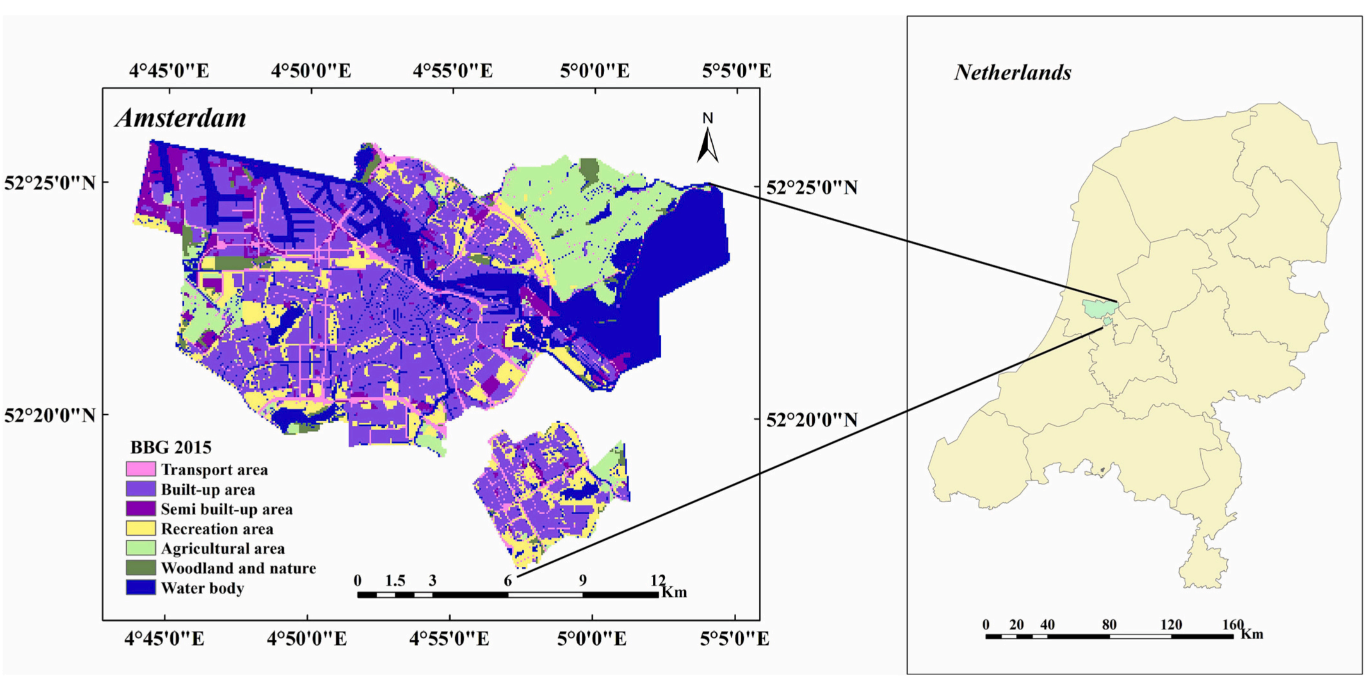

Fig. 1. Location of and land use in Amsterdam.

Table 1
Data input used for assessing the potential food production of Amsterdam's green roofs. Spatial resolution is reported for gridded datasets.

Name	Description	Spatial resolution	Source
Climate data	Daily gridded observational dataset for precipitation, temperature, relative humidity, global radiation, and wind speed.	0.1 arc degrees	(Cornes et al., 2018)
Soil data (rural land)	Soil properties of rural land, including wilting point, field capacity, saturation, and hydraulic conductivity, used to simulate crop yields on rural land for comparison purpose.	1 km	(FAO and IIASA, 2008)
Soil data (green roofs)	Soil properties of a type of lightweight soil used for green roofs, used to simulate crop yields on green roofs.	-	(Ledesma et al., 2022)
Building footprints	Polygons of buildings, also containing the information of roof area, building height, construction year, and building functions.	-	(BAG, 2022)
Digital Surface Model	Contains gridded information of elevation.	0.5 m	(AHN3, 2022)
Aerial image	RGB photo taken in 2017, also used to validate the locations of flat roofs.	25 cm	(NGR, 2017)

areas is available (AHN3, 2022); (ii) it is the most populous city in the Netherlands with close to 900,000 residents in 2022 (CBS, 2022); and (iii) it is highly urbanized, with build-up areas accounting for 48 % of the total land use (Fig. 1, BBG, 2015).

Amsterdam has mild winters, rarely lower than 0 °C, and while the summer is warm, temperatures exceed 30 °C only over a handful of days (KNMI, 2022). The average annual rainfall between 2002 and 2021 was 908 mm (Cornes et al., 2018).

For this study, several datasets were collected from various sources (Table 1). We collected climate and soil data to model crop growth, a map of building footprints to identify the locations of roofs, DSM data to evaluate flat areas on rooftops, and an aerial image to visually validate our interpretation of flat roofs.

2.2. Crop production potential on green roofs

The process to calculate green roofs' crop growth potential consisted of (i) calculating green roof areas, (ii) climate data preprocessing, and (iii) calculating crop growth potential (Fig. 2).

We used daily evapotranspiration (ET0), precipitation, and temperature at 0.1 arc degrees spatial resolution to simulate spatially-differentiated crop yields. We ran our simulations for a typical wet, dry, and average climate year to provide a range of possible yields depending on climate conditions. Dry year, average year, and wet year

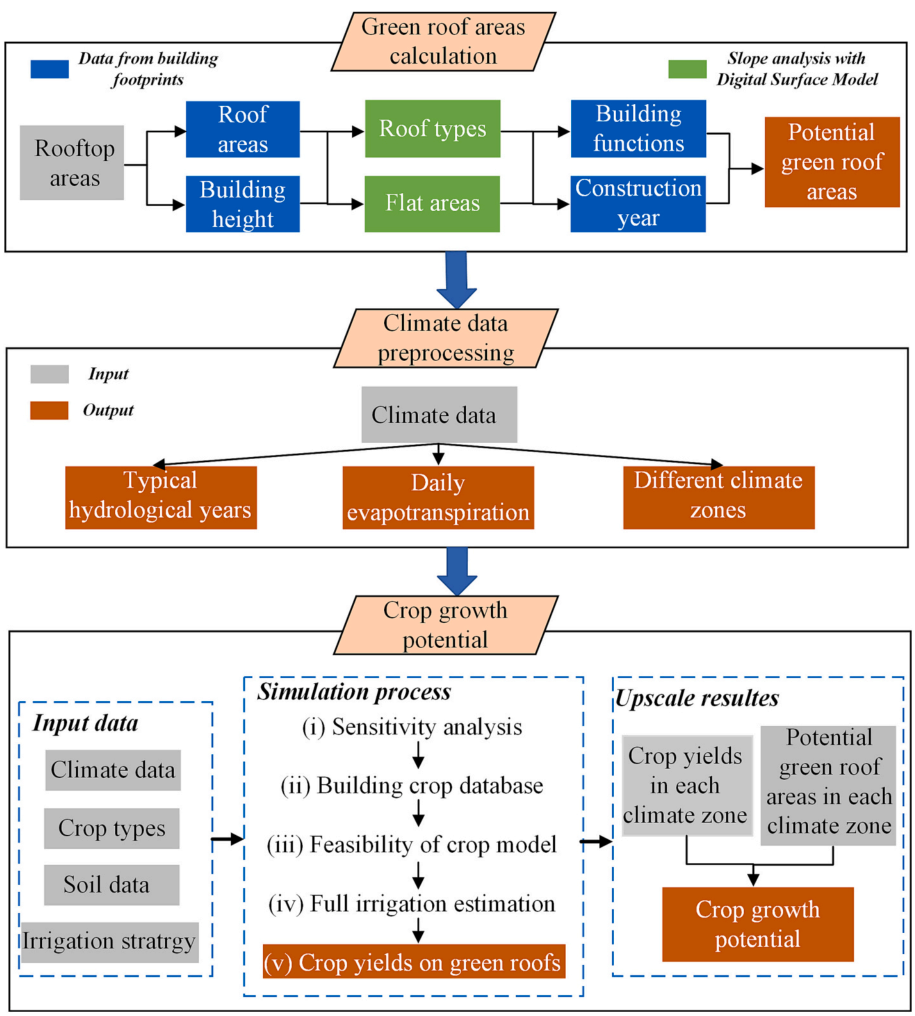

Fig. 2. Modeling steps to calculate crop growth potential from green roofs.

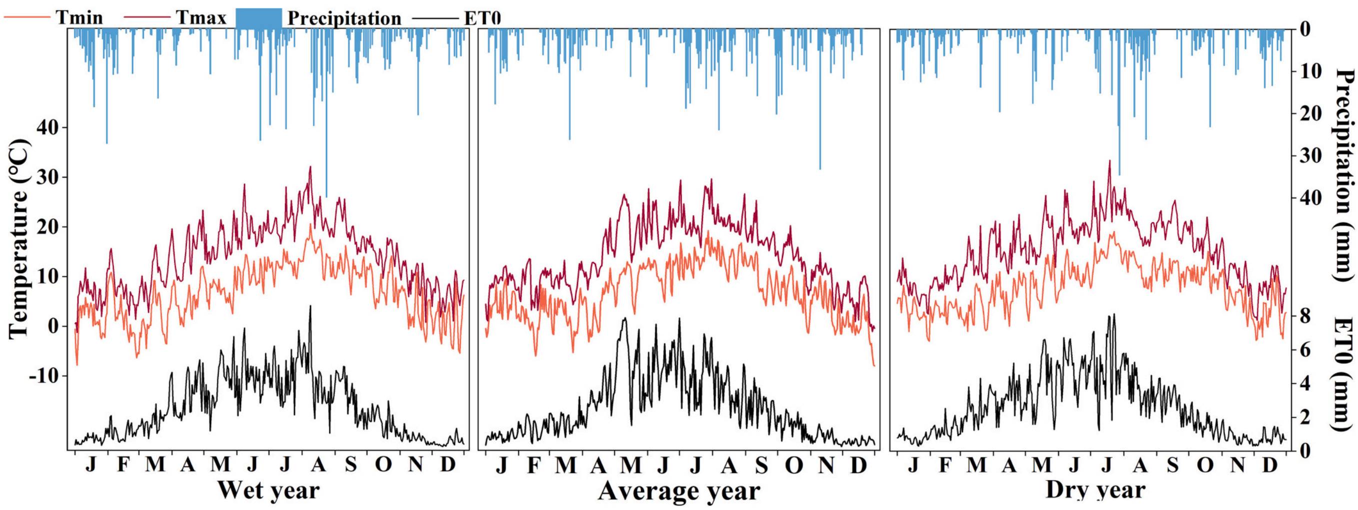

Fig. 3. Precipitation, maximum and minimum temperature, and ET0 daily time series for a) the wet year (2004), b) the average year (2008), and c) the dry year (2014) in Amsterdam. Initials of months are reported on the x-axis.

were determined based on the 1st, 2nd (=median), and 3rd quantiles, respectively, following Lyu et al. (2022). The dry year is represented by 2014 with 867 mm of precipitation, the average year is represented by 2008 with 925 mm of precipitation, and the wet year is represented by 2004 with 974 mm of precipitation (see Fig. S1). Fig. 3 presents daily precipitation, temperature, and ET0 in 2004, 2008 and 2014 in Amsterdam. The data source, description, and values/ranges of the crop database are shown in Tables S1 and S2 in the supplementary materials.

2.3. Green roof area mapping

Rooftop areas suitable for green roofs were determined using several criteria (Table 2). First, we used the DSM (Fig. 4a) to calculate a slope map (Fig. 4b) with the slope tool in ArcGIS 10.7. We then used the polygon boundaries of buildings from the dataset of Basic Registration of Addresses and Buildings (BAG) to determine the rooftop areas (BAG, 2022; Fig. 4c). By combining the slope map with the building polygons, we identified flat rooftop areas (i.e., roof areas with a slope < 10°; Fig. 4d).

After identifying the flat areas on roofs, we considered several other criteria to determine potential green roof areas, which are listed in Table 2.

Table 2
Criteria used to select potential green roof areas.

Criterion	Requirement	Reason
Roof area	A minimum roof area of 13 m^2 (Zambrano-Prado et al., 2021)	Enough roof space is required to install a green roof system.
Available roof area	Roof areas should not be occupied by other objects	Free roof areas are required to install a green roof system
Building height	Above 30 m (Saha and Eckelman, 2017)	Safety considerations due to strong wind on high-rise buildings.
Roof slope	Only flat roof areas are suitable (Zambrano-Prado et al., 2021)	The installation of a green roof system requires a flat surface
Building function	Residential buildings and industrial buildings are not desirable (Shao et al., 2021)	Roofs of industrial buildings do not have enough (> 2 kN/m^2) bearing capacity for a green roof system. Roofs of residential buildings are shared.
Construction year	After 1930 (Silva et al., 2017)	Relatively modern buildings with concrete structure normally show enough (> 2 kN/m^2) bearing capacity (Silva et al., 2017)

We considered three additional steps to refine the suitablity of green roof areas, after mapping flat areas on rooftops (Fig. S2). In the first step, we validate roof types through visual interpretation of aerial imagery. Two image samples with 318 buildings were scanned for flat roofs. Table S3 and Fig. S5 show that a threshold of 34 % of flat areas on one roof was sufficient to distinguish different roof types (91.2 % precision). Therefore, if the value of the threshold is more than 34 %, the roof is identified as a flat roof. In the second step, roof bearing capacity is considered to further exclude additional buildings, following Zambrano-Prado et al., 2021. We exclude industrial buildings and buildings built before 1930 (Table 2). In the last step, we exclude residential buildings due to building ownership (Table 2).

2.4. Crop yield simulations

We used the Aquacrop model to simulate the yield of various crops on green roofs, taking into account the temporal and spatial climatic heterogeneity of Amsterdam. Aquacrop is widely accepted as a valuable tool for simulating crop yield in water-limited environments due to its consideration of water stress, soil-plant-atmosphere interactions, and versatility for a wide range of crops (Steduto et al., 2009). Its user-friendly interface also allows for calculating crop yields on green roofs under different water management strategies.

Five steps were performed for every crop type. (i) A sensitivity analysis of crop parameters, (ii) obtaining a fixed crop database, (iii) validating the feasibility of the Aquacrop model, (iv) determining the irrigation amount, and (v) simulating crop yields on green roofs (Fig. 2).

A Sobol sensitivity analysis combined with the Aquacrop model in Python was used to explore the most sensitive crop parameters with about 320,000 samples for vegetables (taking cabbage as an example). The initial wide ranges of crop parameters are mostly recommended by Aquacrop reference manual book (Steduto et al., 2009). The total order index of 0.01 was set to evaluate the most sensitive crop parameters (Table S4).

After the first step of sensitivity analysis, the crop data were collected to build a database in the second step (Fig. 2). Specifically, the water productivity (WP) was normalized (WP*) for climate situations according to transpiration, actual evapotranspiration, and ET0 of each type of crop in their driest and wettest growth periods. The normalization process follows Eqs. (1)–(3), (Nyathi et al., 2019; Steduto et al., 2009):

$$B = WP^{*} \times \sum_{gp} \left(\frac{T_r}{ET0} \right) \tag{1}$$

$$B = WP \times \sum_{gp} ET_a \tag{2}$$

$$WP^* = WP \times \frac{\sum_{gp} ET_a}{\sum_{gp} \left(\frac{T_r}{ET0}\right)} \tag{3}$$

where B is biomass, WP is water productivity, WP* is normalized water productivity, ETa is actual evapotranspiration, and Tr is transpiration. The goal of the normalization for climate situations is to make WP applicable to diverse locations and seasons. The values of WP* are shown in Table S5.

In the third step, the statistical yield data from the Food and Agriculture Organization of the United Nations (FAO) were used to validate the simulated yields under full irrigation (FI) (FAO, 2022, Fig. 2). FI means the crop will achieve a full yield potential with a certain amount of water resources, normally represented by 80 % field capacity (Liu et al., 2021; Li et al., 2022; Mu et al., 2022).

The fourth step was performed to quantify the FI on green roofs with the new crop database and lightweight soil (Fig. 2). A root-blocking layer was adopted in the green roof systems and Aquacrop model to prevent the rapid root development of crops.

In the last step, optimized regulated deficit irrigation for limited volumes of water (ORDIL) was considered for examining water scarcity to simulate crop yields on green roofs (Fig. 2). The limited available water would be allocated to four growth periods (emergence, canopy growth, max canopy, senescence) of crops to obtain the maximum yield level (Pardo et al., 2022). Here, we took four scenarios of optimized irrigation methods as examples (80 % FI, 60 % FI, 40 % FI, 20 % FI) to see the different yield levels of crops on green roofs.

3. Results

3.1. Potential green roof areas

Overall, flat roofs occupy nearly 1780 ha or 70.9 % of Amsterdam's roof areas, including 26.4 % for non-flat areas (areas already occupied, e.g., solar panels) and 44.5 % for flat areas (Fig. 5b). For the flat areas on flat roofs, 4.45 % represent commercial buildings, 17.80 % public buildings, and 22.44 % other types that are suitable for green roof areas. Ultimately, flat roofs represent 613 ha, with potential green roof areas (those excluding occupied surfaces) occupying 396 ha (Fig. 5a and c).

3.2. Food production potential on green roofs

These results are shown according to the five steps described in the Methods section.

3.2.1. Steps 1 and 2: sensitivity analysis and fixed crop database

Seven parameters out of 18 crop parameters represented the most sensitive crop parameters as their total order index values exceed 0.01: CCx (maximum canopy cover), CGC (canopy growth coefficient), Kcb (crop coefficient), WP* (water productivity normalized for climate situations), HI0 (harvest index), p_up3 (water stress factor) and PlantPop (planting density) (Table S4). HI0 has the highest value of the total order index of 0.34 followed by CCx with a value of 0.28, while the other five sensitive crop parameters have values no more than 0.1. CCx represents the potential size of the crop canopy, which is a critical component of crop growth and yield. HI0 represents the ratio of the weight of harvested crop to the total above-ground biomass of the crop and determines the potential yield of a crop. With this sensitivity information

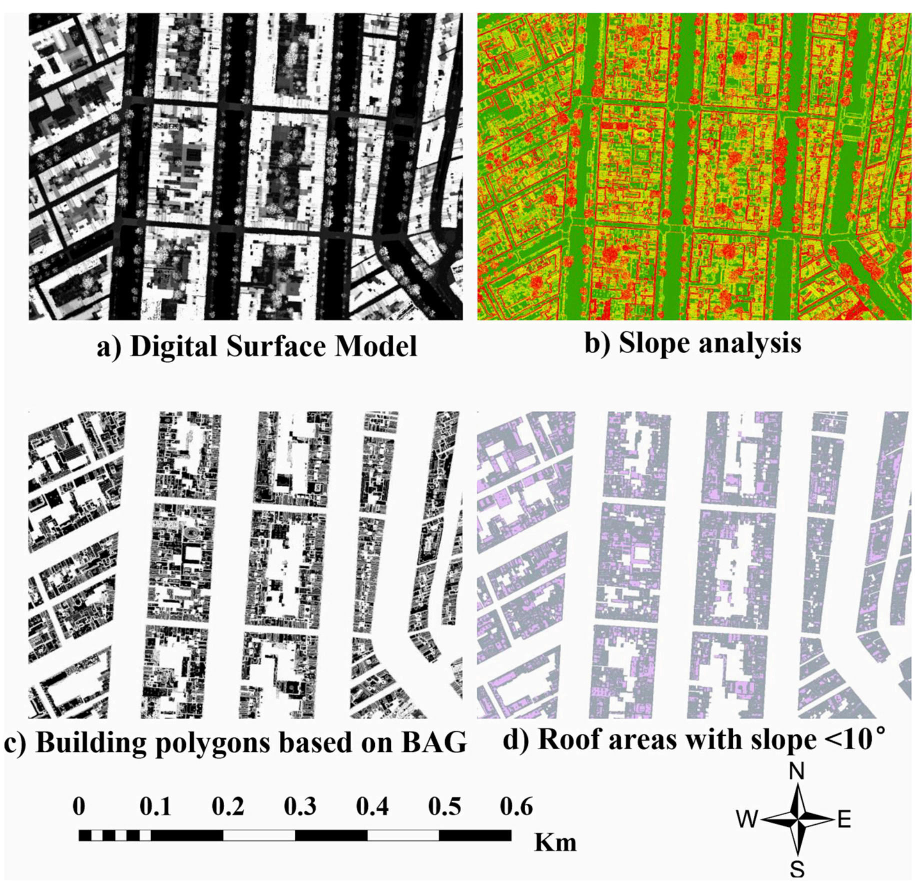

Fig. 4. Steps to identify the flat areas on roofs: a) the Digital Surface Model is used to calculate b) slope values. c) Slopes are then cropped based on building polygons, and d) suitable roof areas are identifies based on the slope threshold.

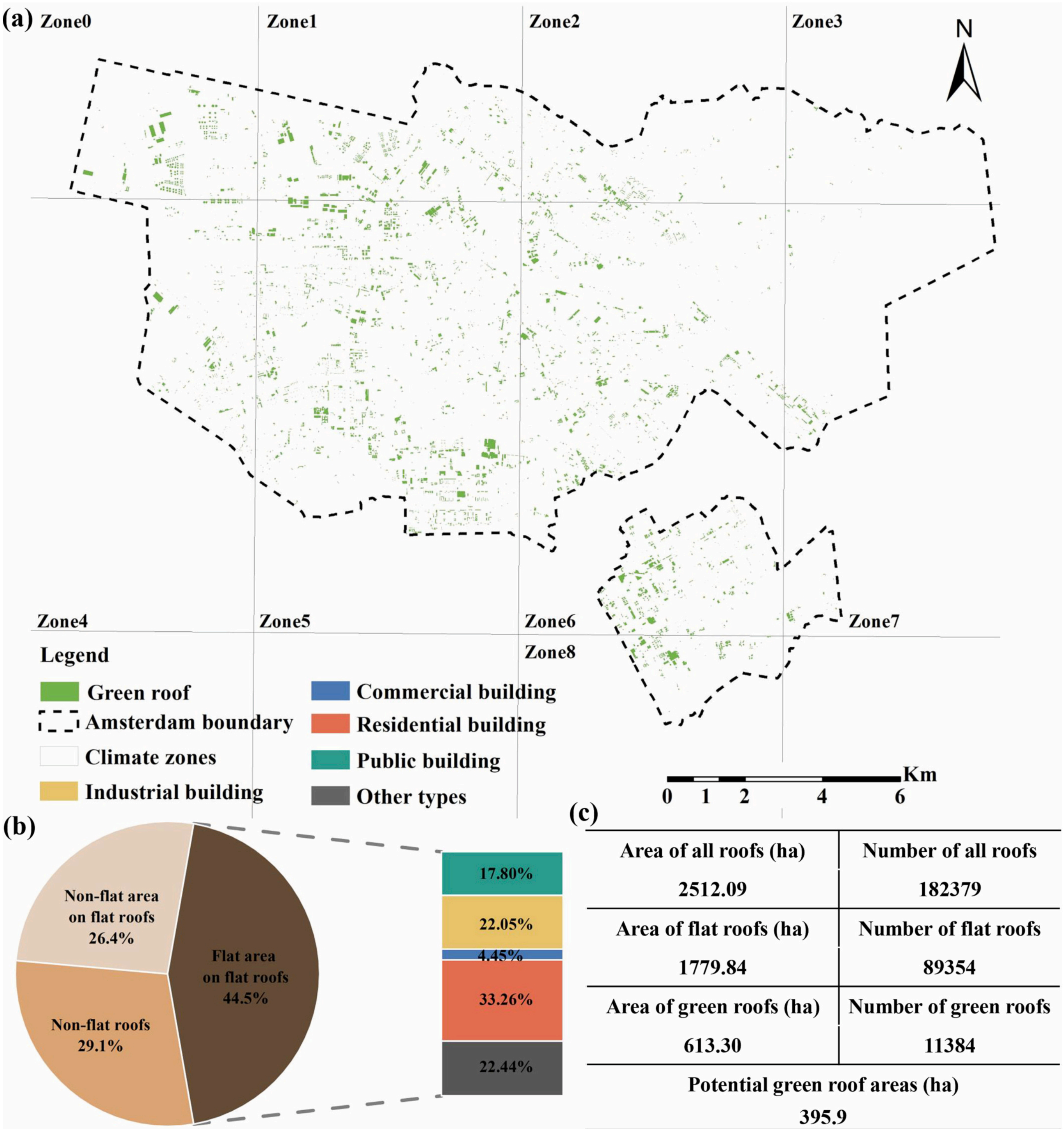

Fig. 5. Description of potential green roof areas and green roofs. a) Location of green roofs in Amsterdam (Zones are divided based on the gridded climate data), b) The proportions of non-flat roofs, non-flat areas on flat roofs, and flat areas on flat roofs dividing different building functions, and c) Estimation of potential green roof areas.

in hand, a crop database for green roof crops in Amsterdam was developed (Table S2). Apart from the ranges of sensitivity parameters, Table S2 also shows the duration of growth periods for different crop varieties.

3.2.2. Step 3: feasibility of Aquacrop model to simulate crop production on roofs

Yield variations for the ten different types of crops (including crop parameter uncertainty) compare well with national yield data from the FAO (Fig. S3). Strawberry yields from FAO increased significantly between 2012 and 2020 and exceeded the highest anticipated yields in 2018. This is because strawberries have a higher production potential in greenhouses than on open-air farmland (CBS, 2022). The almost linear shape in the simulation results between 2002 and 2021 for each type of crop results from the FI irrigation scenario, where yield is less sensitive to irrigation changes. The slight yield increase results from higher CO_2 concentrations over the evaluated timeframe.

3.2.3. Steps 4 and 5: irrigation amount and crop yield

Crop yields vary across different irrigation scenarios and crop types, with some crops showing little variation in yield levels due to sufficient rain-fed soil moisture. The optimal irrigation strategy of 80 % FI could effectively save irrigation water compared with a non-optimized 100 % FI scenario.

We observed a minor difference in FI for each type of crop with different yield levels (Fig. 6a). Leeks had the highest FI (around 300 mm) because they have a longer growth period than other types of crops. For spinach, the FI has a value of 0, indicating a rainfed vegetable without irrigation requirements. Although the FI for cauliflower differs from zero, cauliflower is still a type of rainfed vegetable because there is no yield variance across different irrigation scenarios in Fig. 6b, c, and d. This is because FI merely compensates the soil moisture but is not used for cauliflower growth.

Apart from cauliflower and spinach, similar trends for crop yields under various irrigation strategies occur for most crop types (Fig. 6b, c, and d). When considering the spatial and temporal variability of the climate, the crop yield variance on green roofs for beans is 8.38–17.16 t ha^{-1}, for broccoli is 7.52–29.27 t ha^{-1}, for cabbage is 30.75–75.90 t ha^{-1}, for cauliflower is 7.17–15.74 t ha^{-1}, for leek is 21.30–45.74 t ha^{-1}, for lettuce is 14.77–42.69 t ha^{-1}, for onion is 8.11–26 t ha^{-1}, for pea is 1.74–6.44 t ha^{-1}, for spinach is 2.33–6.57 t ha^{-1}, and for strawberry is 13.11–34.10 t ha^{-1} assuming 100 % FI (Fig. 6). In Fig. 6, the error bars represent yield variance induced by different climate conditions. For instance, spinach's error bars are larger than the error bars for cauliflower, which demonstrates that climate variability across space and time has a greater impact on spinach yields.

The yield levels for bean, broccoli, leek, and onion are quite similar across the 80 % FI and 100 % FI scenarios. This means that and 80 % FI strategy could effectively save irrigation water compared with a 100 % FI strategy. Comparing Fig. 6b, c, and d revealed a significant influence of yield levels on different crops. Yet, the same tendency may also be detected when comparing the yields of different crops in the three figures. The difference in water use efficiency for each variety of crop may be assessed by adding the full irrigation and yield levels. For instance, lettuce has a greater water use efficiency than pea since it yields more while using less water.

Ultimately, Green roofs could produce annually 3.32–6.79 kt for bean, 11.59–29.78 kt for broccoli, 11.98–28.43 kt for cabbage, 2.84–6.23 kt for cauliflower, 8.43–18.11 kt for leek, 5.85–16.90 kt for lettuce, 3.21–10.66 kt for onion, 0.69–2.55 kt for pea, 0.92–2.60 kt for spinach, and 5.19–13.50 kt for strawberry in Amsterdam without inducing scarcity.

Table 3 shows the crop production potential. Cabbage has the largest crop production potential on green roofs in Amsterdam, while pea has the minimum crop production potential under no water scarcity. Fig. S4 and Table S6 also show the crop production on green roofs with irrigation scenarios of 20 %, 40 %, 60 %, and 80 % FI.

4. Discussion

Our results showed a total food production potential of different crops on green roofs in Amsterdam, quantifying this potential by combining a crop growth model (Aquacrop) with spatially-explicit information on green roofs. We found soil type, crop selection, weather conditions, and planting management contribute to crop yield variability on green roofs. The simulated crop yields of bean, broccoli, cabbage, lettuce, and onion generally agree with other studies (Table 4). On green roofs, crop yields could be affected by many factors. For instance, a study by Jing et al. (2021) investigated the impact of temperature and CO_2 concentration on the yields of broccoli and cabbage. They found that these environmental factors significantly affect the productivity of these crops. Similarly, Varela et al. (2021) examined the

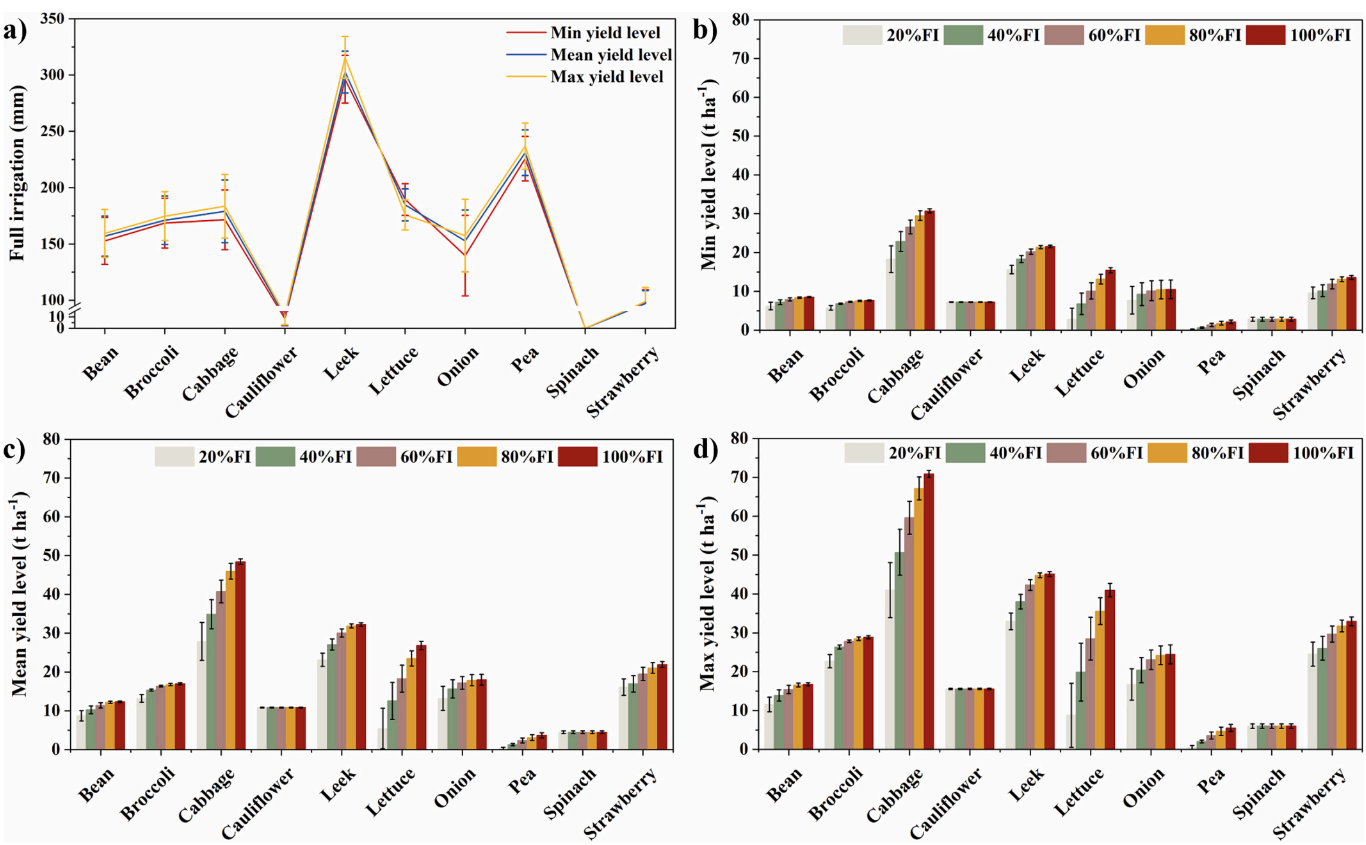

Fig. 6. Full irrigation estimation (a), minimum yield level (b), mean yield level (c), and maximum yield level (d) (Error bar presents the standard error caused by spatial and temporal climate variance).

Table 3
Crop production potential on green roofs without water scarcity considering climate variance (unit: kt y^{-1}).

Crops	Min yield level	Climate variance	Mean yield level	Climate variance	Max yield level	Climate variance
Bean	3.37	±0.05	4.89	±0.08	6.63	±0.16
Broccoli	3.03	±0.05	6.73	±0.10	11.44	±0.15
Cabbage	12.18	±0.20	19.18	±0.28	28.07	±0.36
Cauliflower	2.87	±0.03	4.30	±0.04	6.17	±0.06
Leek	8.56	±0.13	12.76	±0.18	17.87	±0.24
Lettuce	6.11	±0.26	10.63	±0.44	16.23	±0.67
Onion	4.16	±0.95	7.13	±0.56	9.68	±0.98
Pea	0.85	±0.16	1.47	±0.26	2.19	±0.36
Spinach	1.13	±0.21	1.78	±0.14	2.38	±0.22
Strawberry	5.38	±0.19	8.69	±0.30	13.06	±0.44

influence of climatic conditions and substrate types on lettuce yield, revealing that both dry and wet climates, in combination with different substrates, can cause significant yield variance. The effect of cultivar selection and irrigation systems was also demonstrated in a study by Orsini et al. (2014). The study compared the growth of different lettuce cultivars under varied irrigation systems, providing insights into optimal planting management strategies. However, not all studies assess the full crop potential of green roofs. For example, the survey of Uddin (2016) on rooftop garden crop yields underestimated the growth potential of cauliflower and spinach. This was largely due to the low planting density, use of separate containers, and underutilization of rooftop garden areas. Other studies, like that of Richardson et al. (2022), used different cropping systems and cultivars to examine the yield of specific crops like strawberry on green roofs. Similarly, Whittinghill et al. (2013) explored the plant productivity of bean on green roofs, taking into account cropping systems, irrigation strategies, and fertilizer inputs. In conclusion, these studies highlight the myriad of factors that influence crop yields on green roofs, underscoring the need for careful planning and management for optimal productivity.

Compared with previous research estimating the crop yields on green roofs with the statistical data (e.g., FAO and national data), our framework can effectively quantify crop yields under changing environments, such as climate, soil, and planting management (Haberman et al., 2014; Sioen et al., 2017; Weidner and Yang, 2020; Montealegre et al., 2022). Besides, this framework can save time and labor resources with by simulating regional scales in contrast to local experimental measurements (Orsini et al., 2014; Manríquez-Altamirano et al., 2020). Adapting crop models for green roof crop growth presents an opportunity to estimate food production potential across larger urban areas under different changing environments. Our modeling framework can also be extended to analyze the food production potential on green roofs in other cities as well. To use this modeling framework, we require relevant data such as crop information, soil characteristics, planting management data, and climate data. Additionally, building footprints and slope data are essential for estimating the available green roof areas. The accuracy of the results is affected by the precision of the input climate data. This is because spatial variations in climate can impact crop yields across different climate zones.

Table 4
Crop yields on green roofs compared with other studies (unit: t ha^{-1}).

	Current study	Other studies	Region	Source
Bean	8.38–17.16	10.17–15.69	America	(Whittinghill et al., 2013)
Broccoli	7.52–29.27	14.3–23.56	China	(Jing et al., 2021)
Cabbage	30.75–75.90	24.31–112.97	China	(Jing et al., 2021)
Cauliflower	7.17–15.74	0.57	Bangladesh	(Shill et al., 2020, Uddin, 2016)
Leek	21.30–45.74			
Lettuce	14.77–42.69	17.48–28.77	Colombia	(Varela et al., 2021)
		5.00–25.00	Italy	(Orsini et al., 2014)
Onion	8.11–26			
Pea	1.74–6.44			
Spinach	2.33–6.57	0.24	Bangladesh	(Shill et al., 2020, Uddin, 2016)
Strawberry	13.11–34.10	8.8 (planter box) 55.25 (pot)	America	(Richardson et al., 2022)

We used the building functionality and construction year to describe the roof bearing capacity. The assessment of green roof potential requires the specification of urban characteristics such as roof slopes, areas, types, and building functions. These characteristics can be identified using building footprints, aerial photos, and digital surface models. However, information related to load-bearing capacity is not always directly available in these data sources. Load-bearing capacity is a critical factor for determining whether a roof can support a green roof system, and recent studies have focused on exploring methods to describe this capacity. Zambrano-Prado et al. (2021) proposed two approaches to indirectly assess load-bearing capacity. One method involves using hyperspectral data from remote sensors to identify the roof material, which can provide insight into the load-bearing capacity. The other approach assumes that industrial roofs generally have lower load-bearing capacity compared to buildings composed of concrete structures. Silva et al. (2017) suggested using the construction year of a building, specifically 1930, to divide the structural capacity for different construction materials. This approach allows for the estimation of load-bearing capacity by assuming construction material were used in different periods. Nonetheless, when assessing green roof potential, it is essential to consider various urban characteristics to directly or indirectly estimate the load-bearing capacity. These methods can provide valuable insights for determining the feasibility of green roof systems and ensuring their safe and sustainable implementation. To improve our understanding of global green roof potential, spatial datasets should be supplemented with a comprehensive database of building roof-bearing capacities, including any limitations and uncertainties in the estimation. Within this context, and to ensure the safety and long-term sustainability of the green roof system, in cases where direct information on bearing capacity is not available, it is essential to perform roof structure inspections and reinforcement before installing green roof systems.

In our third step we illustrated the variations in crop yields based on national agricultural statistics (FAO statistical data) and compared them with the model results for a range of uncertainty in crop parameters (Fig. S3). The primary purpose of this analysis was to assess the credibility of the collected crop parameter ranges (maximum, mean, minimum) when compared to national crop yield estimates. National crop yield estimates include a large variety of information, including traditional agriculture in rural areas, greenhouse production, hydroponics, and other agricultural techniques that could differ significantly from green roof environments in terms of factors such as substrate composition and management practices. Therefore, our comparisons were a simple aggregated validation with the best data available.

In our study, the modeling framework could also be used as a dynamic tool for forecasting future crop production on green roofs. It can account for potential changes in urbanization rates and shifts in climate patterns. Besides, policymakers can utilize it to pinpoint key green roof criteria that align with specific urban features. This, in turn, aids in the conversion of traditional roofs into productive green spaces. Furthermore, our model can contribute to the development of effective water use strategies, an essential aspect of maximizing crop production on green roofs. As we look to the future, we see a wealth of potential for enhancing the interplay between crop growth and spatial analysis. This could be achieved through the optimization of planting structures on green roofs and considering the diverse crop rotation practices for different crop types. By strengthening this link, we can foster a more nuanced understanding of green roof agriculture. This would pave the way for more efficient and sustainable urban farming practices, contributing to the larger goal of creating sustainable and resilient urban ecosystems.

In an urban environment, leveraging green roofs for crop production has immense potential, but it is crucial that we align this potential with the city's actual crop demand. To achieve this, we need a comprehensive approach that takes into account several key factors. Firstly, we need to assess the total area of green roofs available in the city and identify which crops are most suitable for these spaces, considering factors like local climate and roof structure. Secondly, we need to estimate the yield of these crops per unit area. This provides an idea of the total volume of crops that can be generated. However, this is only addressing supply-side issues. We also need to understand the city's demand for different types of produce. This requires an analysis of local consumption patterns and diets. Combining this demand-side analysis with our supply-side estimates will help us optimize the selection and rotation of crops on green roofs. Moreover, water availability should be taken into account to ensure sustainable practices. Crop choices should reflect water-efficient options suitable for rooftop farming. By following this approach, we can create a more sustainable urban food supply chain, enhancing a city's self-sufficiency in food production. This will not only provide fresh, local produce for residents but also reduce the city's reliance on external food sources, promoting environmental sustainability. In essence, the goal is to integrate urban farming into the city's food system in a manner that is both productive and responsive to local needs. This requires careful planning and an understanding of both the production potential of green roofs and the consumption needs of the city's residents.

5. Conclusion

Taking Amsterdam as a case study, we assessed the crop production potential on green roofs by combining a crop model and a spatial analysis for ten types of shallow-rooted crops. We explored different scenarios of optimized regulated deficit irrigation based on spatial and temporal variance in climate. This research quantifies the crop yields with a productive green roof system through the Aquacrop model, maps the potential green roof areas that are suitable for food production through spatial analysis, and presents crop production as a potential nexus for combining them.

We highlight four main findings. First, green roofs comprise 6.24 % of Amsterdam's total roof count, and these rooftops have the potential to cover 396 ha of green roof areas, equating to 15.8 % of the city's total rooftop space. Second, crop yields on green roofs vary across different crops: beans (8.38–17.2 t ha^{-1}), broccoli (7.52–29.3 t ha^{-1}), cabbage (30.8–75.9 t ha^{-1}), cauliflower (7.17–15.7 t ha^{-1}), leek (21.3–45.7 t ha^{-1}), lettuce (14.8–42.7 t ha^{-1}), onion (8.11–26.0 t ha^{-1}), pea (1.74–6.44 t ha^{-1}), spinach (2.33–6.57 t ha^{-1}), and strawberry (13.1–34.1 t ha^{-1}). Third, the optimized regulated deficit irrigation stands out as an effective strategy for enhancing irrigation management on productive green roofs. Finally, climate variances exhibit diverse effects on crop production under different irrigation scenarios, and irrigation can mitigate the effects of climate variances on food production.

Analyzing crop yields on green roofs aids stakeholders in understanding the agricultural production potential of these rooftop spaces. It also benefits local governments to integrate productive green roofs into urban planting. Crop production on green roofs can help urban food systems become more sustainable and can lead to a greener city.

This framework lays the foundation for future scenario analyses regarding crop production potential on green roofs. Moreover, optimizing planting structures on green roofs should encompass factors such as crop rotations, economic viability, and environmental sustainability. In the future, it is conceivable to establish a comprehensive building database tailored specifically for productive green roof systems.

CRediT authorship contribution statement

Pengxuan Xie: Conceptualization, Methodology, Software, Validation, Visualization, Writing – original draft. **Valerio Barbarossa:** Conceptualization, Methodology, Supervision, Writing – review & editing. **Jan Willem Erisman:** Supervision, Writing – review & editing. **José M. Mogollón:** Conceptualization, Methodology, Supervision, Writing – review & editing.

Declaration of competing interest

The authors declare that there is no conflict of interest exists in the submission of this manuscript.

Data availability

Data will be made available on request.

Acknowledgment

We acknowledge the China Scholarship Council for supporting Pengxuan Xie (file No. 202106300016), and support from Dutch Research Council (NWO) though 'Merian Fund Cooperation China-The Netherlands (CAS) Green Cities 2019' No. 482.19.704. We thank Mike Slootweg for the help provided with the Amsterdam urban spatial data.

Appendix A. Supplementary data

Supplementary data to this article can be found online at https://doi.org/10.1016/j.scitotenv.2023.168051.

References

AHN3 - Het Actueel Hoogtebestand Nederland 3, 2022. https://app.pdok.nl/ahn3-downloadpage/.

BAG - Het Basisregistratie Adressen en Gebouwen, 2022. https://www.pdok.nl/datasets.

BBG - Bestand Bodemgebruik, 2015. https://www.cbs.nl/.

Bren d'Amour, C., Reitsma, F., Baiocchi, G., Barthel, S., Güneralp, B., Erb, K.-H., Haberl, H., Creutzig, F., Seto, K.C., 2017. Future urban land expansion and implications for global croplands. Proc. Natl. Acad. Sci. U. S. A. 114, 8939–8944.

CBS - Statistics Netherlands, 2022. https://www.cbs.nl/.

Clinton, N., Stuhlmacher, M., Miles, A., Uludere Aragon, N., Wagner, M., Georgescu, M., Herwig, C., Gong, P., 2018. A global geospatial ecosystem services estimate of urban agriculture. Earth's Future 6, 40–60.

Cornes, R.C., van der Schrier, G., van den Besselaar, E.J.M., Jones, P.D., 2018. An Ensemble Version of the E-OBS Temperature and Precipitation Data Sets, 123, pp. 9391–9409.

Ćosić, M., Stričević, R., Djurović, N., Moravčević, D., Pavlović, M., Todorović, M., 2017. Predicting biomass and yield of sweet pepper grown with and without plastic film mulching under different water supply and weather conditions. Agric Water Manag 188, 91–100.

FAO, 2018. The Future of Food and Agriculture – Alternative Pathways to 2050. Rome. (224 pp.).

FAO - Food and Agriculture Organization of the United Nations, 2022. https://www.fao.org/faostat.

FAO, IIASA, 2008. China Soil Map Based Harmonized World Soil Database (HWSD). Food and Agriculture Organization of the United Nations, International Institute for Applied Systems Analysis. http://westdc.westgis.ac.cn/.

Foley, J.A., Ramankutty, N., Brauman, K.A., Cassidy, E.S., Gerber, J.S., Johnston, M., Mueller, N.D., O'Connell, C., Ray, D.K., West, P.C., Balzer, C., Bennett, E.M., Carpenter, S.R., Hill, J., Monfreda, C., Polasky, S., Rockstrom, J., Sheehan, J., Siebert, S., Tilman, D., Zaks, D.P., 2011. Solutions for a cultivated planet. Nature 478, 337–342.

Getter, K.L., Rowe, D.B., 2006. The role of extensive green roofs in sustainable development. HortScience 41, 1276–1285.

Godfray, H.C.J., Beddington, J.R., Crute, I.R., Haddad, L., Lawrence, D., Muir, J.F., Pretty, J., Robinson, S., Thomas, S.M., Toulmin, C., 2010. Food security: the challenge of feeding 9 billion people. Science 327, 812–818.

Haberman, D., Gillies, L., Canter, A., Rinner, V., Pancrazi, L., Martellozzo, F., 2014. The potential of urban agriculture in Montréal: a quantitative assessment. ISPRS Int. J. Geo Inf. 3, 1101–1117.

Han, C., Zhang, B., Chen, H., Liu, Y., Wei, Z., 2020. Novel approach of upscaling the FAO AquaCrop model into regional scale by using distributed crop parameters derived from remote sensing data. Agric Water Manag 240.

Jing, R., Li, Y., Wang, M., Chachuat, B., Lin, J., Guo, M., 2021. Coupling biogeochemical simulation and mathematical optimisation towards eco-industrial energy systems design. Appl. Energy 290.
Ket, P., Garré, S., Oeurng, C., Hok, L., Degré, A., 2018. Simulation of crop growth and water-saving irrigation scenarios for lettuce: a monsoon-climate case study in Kampong Chhnang, Cambodia. Water 10.
KNMI - Royal Netherlands Meteorological Institute, 2022. https://www.knmi.nl/over-het-knmi/about.
Ledesma, G., Nikolic, J., Pons-Valladares, O., 2022. Co-simulation for thermodynamic coupling of crops in buildings. Case study of free-running schools in Quito, Ecuador. Build. Environ. 207.
Li, X., Zhang, H., Li, F., Deng, H., Wang, Z., Chen, X., 2022. Evaluating effects of regulated deficit irrigation under mulched on yield and quality of pumpkin in a cold and arid climate. Water 14.
Liu, X., Yang, D., 2021. Irrigation schedule analysis and optimization under the different combination of P and ET0 using a spatially distributed crop model. Agric Water Manag 256.
Liu, N., Fan, X., Cao, X., Zhang, Y., Tian, Y., Cheng, Y., Hao, L., Chen, W., He, C., Yan, R., Chang, Z., Zheng, Y., 2021. Elevated CO2 concentration alleviates the adverse effects of drought stress by modifying stomatal traits of green pepper (Capsicum annuum L.). Pol. J. Environ. 30 (6), 5605–5615.
Lyu, J., Jiang, Y., Xu, C., Liu, Y., Su, Z., Liu, J., He, J., 2022. Multi-objective winter wheat irrigation strategies optimization based on coupling AquaCrop-OSPy and NSGA-III: a case study in Yangling, China. Sci. Total Environ. 843, 157104.
Manivasagam, V.S., Rozenstein, O., 2020. Practices for upscaling crop simulation models from field scale to large regions. Comput. Electron. Agric. 175.
Manríquez-Altamirano, A., Sierra-Pérez, J., Muñoz, P., Gabarrell, X., 2020. Analysis of urban agriculture solid waste in the frame of circular economy: case study of tomato crop in integrated rooftop greenhouse. Sci. Total Environ. 734, 139375.
Meng, F., Yuan, Q., Bellezoni, R., de Oliveira, J.P., Hu, Y., Jing, R., Liu, G., Yang, Z., Seto, K., 2022. A method to analyze the food-water-energy nexus for data-sparse cities: a comparison of green roofs in São José dos Campos, Brazil and Johannesburg, South Africa. 27 September 2022, PREPRINT (Version 1) available at Res. Square. https://doi.org/10.21203/rs.3.rs-1964078/v1.
Meng, F., Yuan, Q., Bellezoni, R.A., de Oliveira, J.A.P., Cristiano, S., Shah, A.M., Liu, G., Yang, Z., Seto, K.C., 2023. Quantification of the food-water-energy nexus in urban green and blue infrastructure: a synthesis of the literature. Resour. Conserv. Recycl. 188.
Montealegre, A.L., Garcia-Perez, S., Guillen-Lambea, S., Monzon-Chavarrias, M., Sierra-Perez, J., 2022. GIS-based assessment for the potential of implementation of food-energy-water systems on building rooftops at the urban level. Sci. Total Environ. 803, 149963.
Mu, Q., Xu, J., Yu, M., Guo, Z., Dong, M., Cao, Y., Zhang, S., Sun, S., Cai, H., 2022. Physiological response of winter wheat (Triticum aestivum L.) during vegetative growth to gradual, persistent and intermittent drought. Agric. Water Manag. 274.
Nadal, A., Alamus, R., Pipia, L., Ruiz, A., Corbera, J., Cuerva, E., Rieradevall, J., Josa, A., 2017. Urban planning and agriculture. Methodology for assessing rooftop greenhouse potential of non-residential areas using airborne sensors. Sci. Total Environ. 601-602, 493–507.
NGR – Nationaal Georegister, 2017. https://data.nlextract.nl/beeldmateriaal/.
Nyathi, M.K., Mabhaudhi, T., Van Halsema, G.E., Annandale, J.G., Struik, P.C., 2019. Benchmarking nutritional water productivity of twenty vegetables - a review. Agric Water Manag 221, 248–259.
Orsini, F., Gasperi, D., Marchetti, L., Piovene, C., Draghetti, S., Ramazzotti, S., Bazzocchi, G., Gianquinto, G., 2014. Exploring the production capacity of rooftop gardens (RTGs) in urban agriculture: the potential impact on food and nutrition security, biodiversity and other ecosystem services in the city of Bologna. Food Secur. 6, 781–792.
Pardo, J.J., Sánchez-Virosta, A., Léllis, B.C., Domínguez, A., Martínez-Romero, A., 2022. Physiological basis to assess barley response to optimized regulated deficit irrigation for limited volumes of water (ORDIL). Agric Water Manag 274, 107917.
Paredes, P., Torres, M.O., 2016. Parameterization of AquaCrop model for vining pea biomass and yield predictions and assessing impacts of irrigation strategies considering various sowing dates. Irrig. Sci. 35, 27–41.
Pérez-Ortolá, M., Daccache, A., Hess, T.M., Knox, J.W., 2014. Simulating impacts of irrigation heterogeneity on onion (Allium cepa L.) yield in a humid climate. Irrig. Sci. 33, 1–14.
Richardson, M.L., Arlotta, C.G., Lewers, K.S., 2022. Yield and nutrients of six cultivars of strawberries grown in five urban cropping systems. Sci. Hortic. 294, 110775.
Saha, M., Eckelman, M.J., 2017. Growing fresh fruits and vegetables in an urban landscape: a geospatial assessment of ground level and rooftop urban agriculture potential in Boston, USA. Landsc. Urban Plan. 165, 130–141.
Shao, H., Song, P., Mu, B., Tian, G., Chen, Q., He, R., Kim, G., 2021. Assessing city-scale green roof development potential using Unmanned Aerial Vehicle (UAV) imagery. Urban Forest. Urban Green. 57.
Shill, L.C., Sarkar, P., Habib, M.A., Purba, N.H., Sarkar, C., Eashat, M.F.S., Chowdhury, M.H., 2020. Rooftop gardening to improve food security in Dhaka city: a review of the present practices. Int. Multidiscip. Res. J. 17–21.
Silva, C.M., Flores-Colen, I., Antunes, M., 2017. Step-by-step approach to ranking green roof retrofit potential in urban areas: a case study of Lisbon, Portugal. Urban For. Urban Green. 25, 120–129.
Sioen, G.B., Sekiyama, M., Terada, T., Yokohari, M., 2017. Post-disaster food and nutrition from urban agriculture: a self-sufficiency analysis of Nerima Ward, Tokyo. Int. J. Environ. Res. Public Health 14.
Smit, J., Nasr, J., Ratta, A., 1996. Urban Agriculture: Food, Jobs and Sustainable Cities, New York, USA.
Steduto, P., Hsiao, T.C., Raes, D., Fereres, E., 2009. AquaCrop—the FAO crop model to simulate yield response to water: I. Concepts and underlying principles. Agron. J. 101, 426–437.
Tian, X., Engel, B.A., Qian, H., Hua, E., Sun, S., Wang, Y., 2021. Will reaching the maximum achievable yield potential meet future global food demand? J. Clean. Prod. 294, 126285.
Uddin, J., 2016. Baseline Study on Roof Top Gardening in Dhaka and Chittagong City of Bangladesh Enhancing Urban Horticulture Production to Improve Food and Nutrition Security (TCP/BGD/3503).
Varela, A., Sandoval-Albán, A., Muñoz, M., Gómez Gómez, A., Bogoya, J.M., Combariza, G., 2021. Evaluation of green roof structures and substrates for Lactuca sativa L. in tropical conditions. Urban Forest. Urban Green. 60, 127063.
Weidner, T., Yang, A., 2020. The potential of urban agriculture in combination with organic waste valorization: assessment of resource flows and emissions for two european cities. J. Clean. Prod. 244.
Wellens, J., Raes, D., Traore, F., Denis, A., Djaby, B., Tychon, B., 2013. Performance assessment of the FAO AquaCrop model for irrigated cabbage on farmer plots in a semi-arid environment. Agric Water Manag 127, 40–47.
Whittinghill, L.J., Rowe, D.B., Cregg, B.M., 2013. Evaluation of vegetable production on extensive green roofs. Agroecol. Sustain. Food Syst. 37, 465–484.
Zambrano-Prado, P., Muñoz-Liesa, J., Josa, A., Rieradevall, J., Alamús, R., Gasso-Domingo, S., Gabarrell, X., 2021. Assessment of the food-water-energy nexus suitability of rooftops. A methodological remote sensing approach in an urban Mediterranean area. Sustain. Cities Soc. 75.